Micro-electrical discharge machining of 3D micro-molds from $Pd_{40}Cu_{30}P_{20}Ni_{10}$ metallic glass by using laminated 3D micro-electrodes

2016 J. Micromech. Microeng. 26 035004

(http://iopscience.iop.org/0960-1317/26/3/035004)

J. Micromech. Microeng. **26** (2016) 035004 (10pp) doi:10.1088/0960-1317/26/3/035004

Micro-electrical discharge machining of 3D micro-molds from $Pd_{40}Cu_{30}P_{20}Ni_{10}$ metallic glass by using laminated 3D micro-electrodes

Bin Xu[1], Xiao-yu Wu[1], Jiang Ma[1], Xiong Liang[1], Jian-guo Lei[1], Bo Wu[1], Shuang-chen Ruan[2] and Zhen-long Wang[3]

[1] Shenzhen Key Laboratory of Advanced Manufacturing Technology for Mold&Die, Shenzhen University, Shenzhen 518060, People's Republic of China
[2] Shenzhen Key Laboratory of Laser Engineering, Shenzhen University, Shenzhen 518060, People's Republic of China
[3] School of Mechatronics Engineering, Harbin Institute of Technology, Harbin 150001, People's Republic of China

E-mail: wuxy@szu.edu.cn and ljg_sc111@163.com

Received 2 September 2015, revised 21 December 2015
Accepted for publication 6 January 2016
Published 27 January 2016

Abstract
For obtaining 3D micro-molds with better surface quality (slight ridges) and mechanical properties, in this paper 3D micro-electrodes were fabricated and applied to micro-electrical discharge machining (micro-EDM) to process $Pd_{40}Cu_{30}P_{20}Ni_{10}$ metallic glass. First, 100 μm-thick Cu foil was cut to obtain multilayer 2D micro-structures and these were connected to fit 3D micro-electrodes (with feature sizes of less than 1 mm). Second, under the voltage of 80 V, pulse frequency of 0.2MHZ, pulse width of 800 ns and pulse interval of 4200 ns, the 3D micro-electrodes were applied to micro-EDM for processing $Pd_{40}Cu_{30}P_{20}Ni_{10}$ metallic glass. The 3D micro-molds with feature within 1 mm were obtained. Third, scanning electron microscope, energy dispersive spectroscopy and x-ray diffraction analysis were carried out on the processed results. The analysis results indicate that with an increase in the depth of micro-EDM, carbon on the processed surface gradually increased from 0.5% to 5.8%, and the processed surface contained new phases ($Ni_{12}P_5$ and Cu_3P).

Keywords: 3D micro-electrode, micro-EDM, 3D micro-mold, metallic glass

(Some figures may appear in colour only in the online journal)

1. Introduction

In recent years, with the development of microelectromechanical systems (MEMS) and precision machinery, the demand for micro-parts in the industrial field has grown exponentially. Micro-electrical discharge machining (micro-EDM) is a common technique for machining micro-parts, characterized by its small cutting force and ability to process a variety of super-hard and brittle materials. Based on these aforementioned advantages, micro-EDM has been widely applied for processing micro-holes, micro-parts and micro-molds.

Considering the difficulty of preparing 3D micro-electrodes, a micro-electrode with a simple cross-section is usually used in micro-EDM to process the 3D microstructures through layer by layer electro-discharge machining. In order to prepare complex 3D micro-structures, Yu *et al* proposed the uniform wear method (UWM) [1]. For realizing arbitrary 3D microstructure processing, Rajurkar and Yu combined the computer aided design (CAD)/computer aid manufacturing (CAM) system with the UWM in micro-EDM [2]. The UWM is a good method for processing 3D microstructures despite its low machining efficiency. To improve the efficiency of 3D micro-EDM, Li and Tong put forward the servo

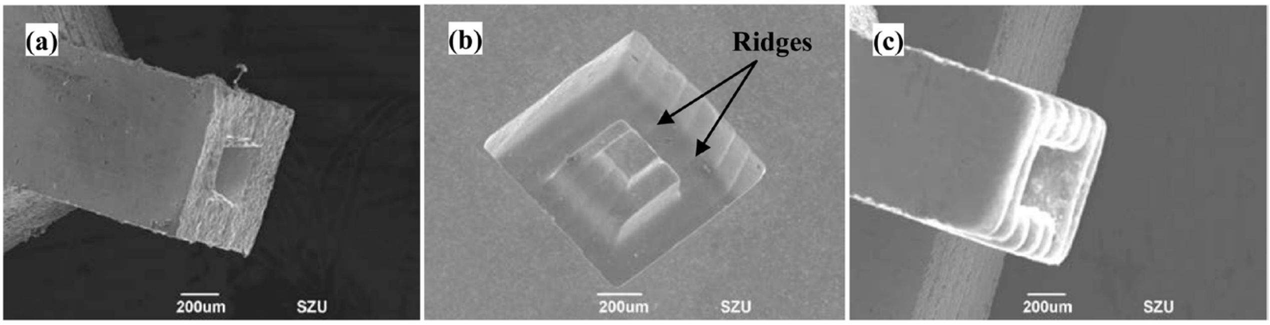

Figure 1. Application of a 3D micro-electrode in micro-EDM from 304# stainless steel: (a) 3D micro-electrode before micro-EDM; (b) 3D microstructure obtained from micro-EDM and ridges on its surface; (c) 3D micro-electrode after micro-EDM and its wear.

scanning 3D micro-EDM (3D SSMEDM) method, in which electrode wear is compensated in real time [3, 4]. The 3D SSMEDM effectively improved the efficiency of 3D micro-EDM and promoted the application of the process in industry. For the purpose of preparing 3D spiral microstructures, Chi and Wang came up with the micro-reversible EDM [5, 6], which expands the processing scope of micro-EDM.

Directed at the electrode wear in 3D micro-EDM, Yu *et al* proposed a new tool wear compensation method (CLU), which combined the linear compensation method (LCM) with UWM [7]. The CLU improved the machining precision, surface quality and machining efficiency of 3D micro-EDM. With the purpose of improving the machining precision of 3D micro-EDM, Nguyen *et al* identified and analyzed the error components of the 3D micro-EDM milling process [8]. By using this method, Nguyen *et al* processed 3D microstructures with a machining error less than 1 μm. In order to obtain accurate electrode compensation, Yan *et al* applied the machine vision system to micro-EDM and prepared high-precision 3D microstructures through doing so [9]. By using this method, the *X*–*Y* geometrical errors of machined structures can be controlled within 10 μm. Similarly, Bleys *et al* also proposed the real-time electrode wear compensation method and prepared 3D micro cavity structures [10]. With this method, tool wear is continuously evaluated during machining and the actual wear compensation is adapted on the basis of this real-time wear evaluation. For fabricating concave and mushroom-shaped spherical structures, Li *et al* proposed a 3D process based on micro-ultrasonic machining (micro-USM), lapping and micro-EDM [11]. As a result of this method, the tool wear ratio is within 5% and the mushroom-shaped spherical structures (with 1 mm diameter) were fabricated in N-BK7 optical glass. To enhance the performance of micro-wire electronic discharge machining (WEDM), Chen and Chen designed a pluri resistance–capacitance (pRC) circuit [12]. This novel power source based on a pRC circuit successfully fabricated a rook-shaped structure and high-aspect-ratio microstructure. In order to fabricate micro-holes at the end of a slim electrode and circulate the dielectric fluid from the other end, Shibayama and Kunieda proposed fabricating the tool electrode with micro-holes by diffusion bonding [13]. The basic idea of this work provided a good reference for fabricating the 3D micro-electrodes.

The above studies mainly use micro-electrodes with a simple cross-section to process 3D microstructures by using the layer-by-layer scan machining method. This processing method has shortcomings such as serious electrode wear and low processing efficiency. If 3D micro-electrodes can be used for 3D micro-EDM, then 3D microstructures can be obtained with an up and down reciprocating machining method, which can improve the machining efficiency of the 3D micro-cavity mold.

In previous work, we fabricated 3D micro-electrodes and applied them to process 304# stainless steel with micro-EDM [14, 15]. From the machining result shown in figure 1, there are some ridges on the surface of the 3D micro-molds. These ridges can influence the surface quality and shape accuracy of the micro-molds, which should be avoided. Metallic glass has good mechanical properties such as high intensity, hardness, abrasive resistance and corrosion resistance. It is difficult to process by the traditional machining method and usually completed by EDM and hot embossing [16]. Compared with 304# stainless steel, the $Pd_{40}Cu_{30}P_{20}Ni_{10}$ metallic glass has a bigger Vickers hardness (510.75Hv) and fracture strength (1326 MPa). Therefore, metallic glass is an ideal material to process 3D micro-molds with better mechanical properties.

In this paper, in order to obtain 3D micro-molds with better mechanical properties, the 3D micro-electrode was applied in micro-EDM for processing $Pd_{40}Cu_{30}P_{20}Ni_{10}$ metallic glass. Moreover, obtaining 3D micro-molds with a good surface quality (slight ridges) is another purpose of this paper.

2. Fabrication process of 3D micro-electrode

Fabricating 3D micro-electrodes mainly includes WEDM station and vacuum pressure thermal diffusion welding station, which is called micro double-staged laminated object manufacturing (micro-DLOM) [14, 15]. A sketch of the process of fabricating 3D micro-electrodes with micro-DLOM process is shown in figure 1 and the specific process is described as follows:

(1) According to the 3D micro-mold model, the 3D micro-electrode model is created. This is then sliced along its height by CAD slicing software to obtain the laminated micro-electrode model (figure 2(a)).

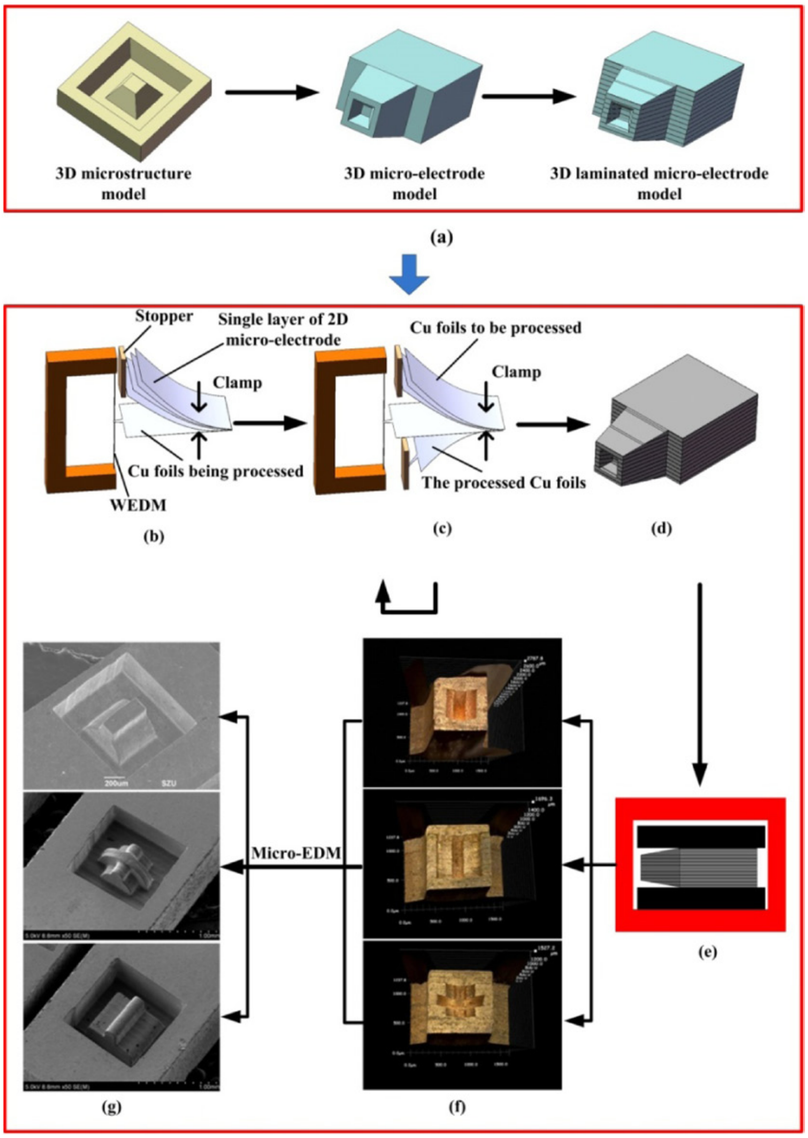

Figure 2. A sketch of the process of fabricating 3D micro-electrodes. (a) Design of the 3D laminated micro-electrode. (b) Fabrication of the first layer of the 2D micro-electrode. (c) Fabrication of the interlayer 2D micro-electrode. (d) Preliminarily laminated 3D micro-electrode. (e) Vacuum pressure thermal diffusion welding. (f) The 3D micro-electrode. (g) The 3D micro-structure.

(2) The multi-layer Cu foils determined in step (1) are clamped by fixture and cut by WEDM (figures 2(b) and (c)). Cu foils consist of processed foils, foils that are being processed andfoils to be processed (figures 2(b) and (c)). During the fabrication of the 3D micro-electrode, the other end of the Cu foils that are being processed should be fixed by a magnet holder and this layer of foil is processed by WEDM to obtain the 2D micro-structure. At the same time, by using a stopper, the other end of the Cu foils to be processed and the processed Cu foils are bent upward and downward respectively (figure 2(c)). The above process is repeated until each layer of the 2D micro-structure is obtained. The preliminarily laminated 3D micro-electrode is then fitted (figure 2(d)).

(3) Each layer of 2D microstructure in the preliminarily laminated 3D micro-electrode is not actually connected. Therefore, the preliminarily laminated 3D micro-electrode should be placed in a vacuum furnace and vacuum pressure thermal diffusion welding performed (figure 2(e)). After that, each layer of the 2D micro-structure in the preliminarily laminated 3D micro-electrode can achieve full connection.

(4) The 3D micro-electrode (figure 2(f)) which is obtained by the micro-DLOM process is applied to micro-EDM and the 3D micro-mold can be obtained (figure 2(g)).

3. Experimental materials and equipment

100 μm-thick copper foil was used to fabricate the 3D micro-electrode. The metallic glass is composed of Pd, Ni, Cu and P, and their atomic percentages are 40%, 10%, 30% and 40% respectively. The equipment and schematic adopted in this paper is shown in figure 3. The wire cutting machine is a middle-speed WEDM (Model: H-CUT32F), manufactured by HI-LINK Precision Machinery Co., Ltd. The furnace is a

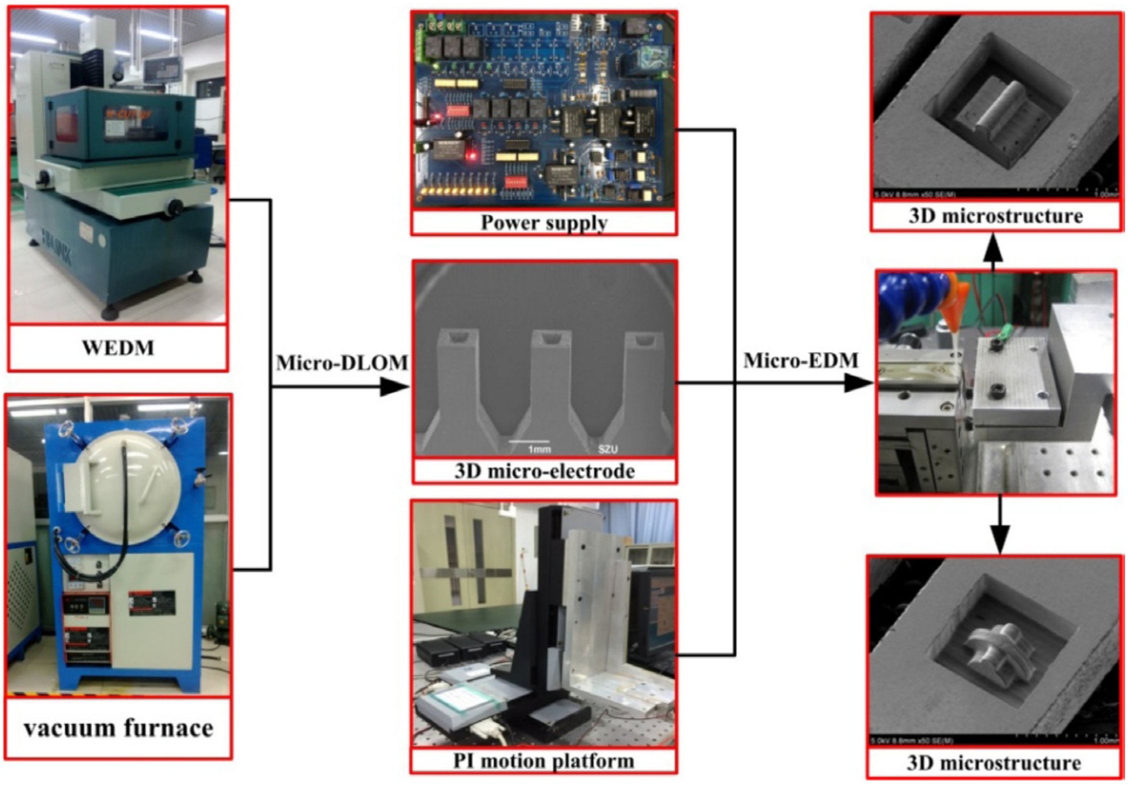

Figure 3. The experimental facilities used in this study.

vacuum heat treatment furnace (Model: ZK1-12–1200), manufactured by Shenzhen Zhongda Electric Furnace Factory. A high-precision motion platform (Model: M511.DD) produced by the company German Physik Instrumente was used to establish an experimental platform for micro-EDM. A laser scanning confocal microscope (model: VK-X100) produced by the company KEYENCE was used to measure the surface roughness of 3D micro-mold. The digital microscope (model: VHX-1000) produced by KEYENCE company was used to observe the 3D microelectrode and 3D micro-mold. The scanning electron microscope (Model: SU-70) produced by Hitachi company was used to observe the surface topography of micro-mold and carry out EDS analysis. An x-ray diffractometer (Model: D8 Advance) produced by BRUKER AXS was used to carry out XRD testing.

4. Results and discussions

4.1. Fabrication of 3D micro-electrode and 3D micro-mold

Using 100 μm-thick copper foil as the raw material, the 3D micro-electrodes were fabricated by WEDM and a vacuum furnace. The process parameters for fabricating the 3D micro-electrode are as follows: wire-cutting current of 0.42 A, wire-cutting voltage of 80V, pulse width of 10 μs, pulse interval of 40 μs, thermal diffusion temperature of 850 °C, thermal diffusion time of 10 h and pressure of 100 N.

Cu foils are the raw material for fabricating the 3D micro-electrode and there are some CuO and impurities adhering to the surface of Cu foil. Through vacuum pressure thermal diffusion welding, multi-layer Cu foils were connected together and the 3D micro-electrode can be obtained. Under the influence of CuO and impurities, the resistance of 3D micro-electrode is inhomogeneous. The resistance R_0 between each layer of Cu foil is bigger than the resistance R in other places. Therefore, when the 3D micro-electrode is applied to micro-EDM, the wear between each layer of Cu foil is greater than in other places (figure 1(c)). As a result, the inhomogeneity of wear in the 3D micro-electrode could cause the ridges on the surface of the 3D microstructure (figure 1(b)). So, by using a 3D micro-electrode in micro-EDM, the ridges on the surface of 3D microstructure are inevitable.

The wear of 3D micro-electrode is closely related to the resistivity of the processing material when the electrode material, dielectric and machining voltage are determined. Under the effect of machining voltage, heat is generated between the electrode and the processing material. With the action of the generated heat, the processing material is removed and the electrode is worn. The generated heat is related to the interelectrodes current. Under the effect of the same electrode, dielectric and machining voltage, the processing material with higher resistivity will be processed by the smaller interelectrodes current and thus the wear of 3D micro-electrode is decreased accordingly. The resistivity of 304# stainless steel is 0.73×10^{-6} Ω·m and the resistivity of $Pd_{40}Cu_{30}P_{20}Ni_{10}$ metallic glass is $0.26 \times 10^{-3}\Omega$·m. Therefore, under the effect of the same electrode, dielectric and machining voltage, the wear of 3D micro-electrodes is smaller when the 3D micro-electrode is applied for processing $Pd_{40}Cu_{30}P_{20}Ni_{10}$ metallic glass. Consequently, applying a 3D micro-electrode for

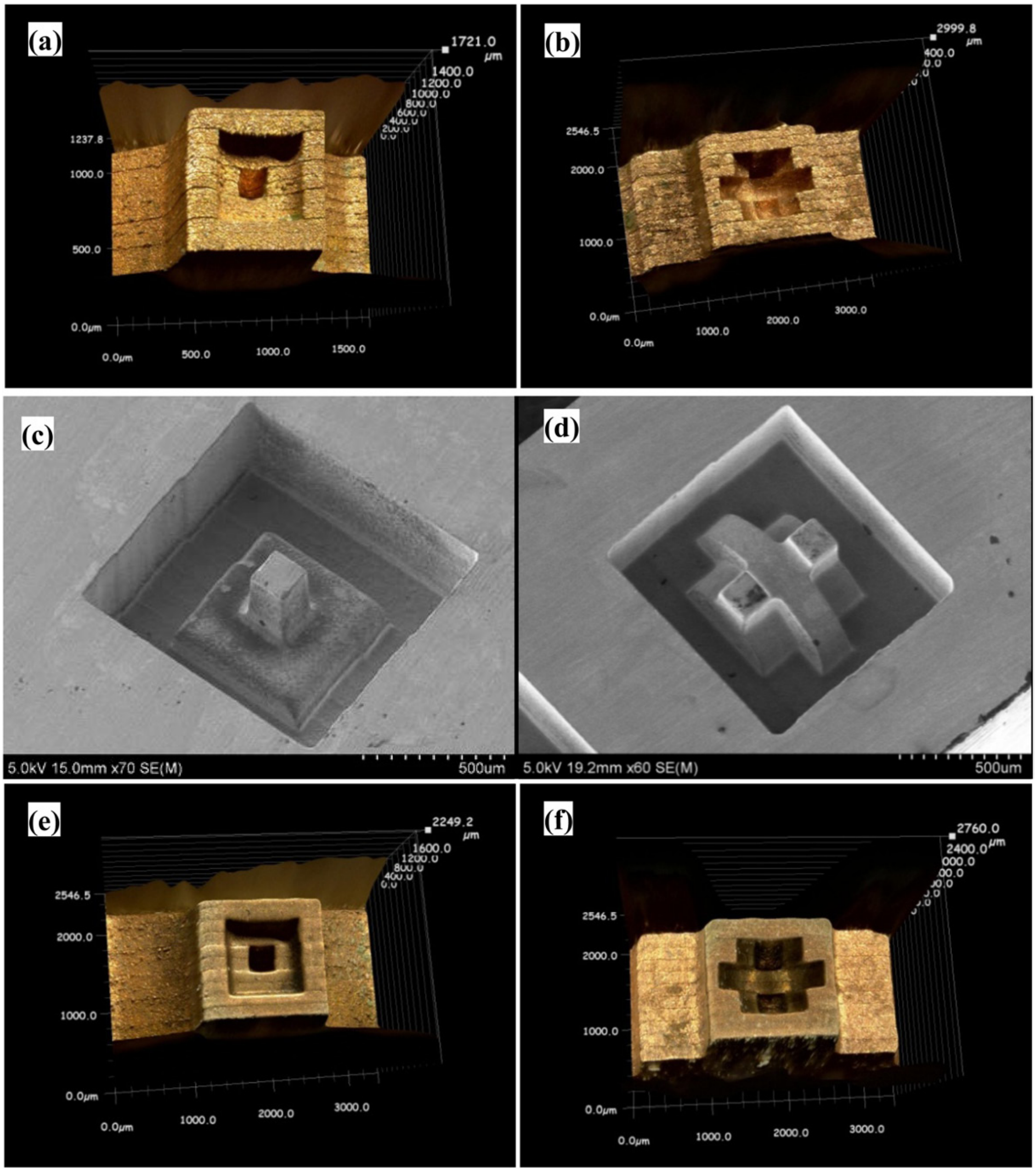

Figure 4. The 3D micro-electrode and 3D micro-mold: (a), (b) 3D micro-electrodes before micro-EDM; (c), (d) the SEM photos of 3D micro-molds; (e), (f) 3D micro-electrodes after micro-EDM.

processing $Pd_{40}Cu_{30}P_{20}Ni_{10}$ metallic glass, the ridges on the surface of 3D microstructure are slight.

3D micro-electrodes were used to carry out micro-EDM on $Pd_{40}Cu_{30}P_{20}Ni_{10}$ metallic glass and 3D micro-molds were obtained. The parameters for the micro-EDM were as follows: voltage of 80 V, pulse frequency of 0.2 MHz, pulse width of 800 ns and pulse interval of 4200 ns. The 3D micro-electrodes were observed by the digital microscope and their 3D images were obtained. These images are shown in figures 4(a), (b), (e) and (f). The 3D micro-molds were observed by SEM and the results are shown in figures 4(c) and (d). From the experimental results, it can be seen that the 3D micro-mold has good surface morphology, approximately in line with the design model. The processing time of the 3D micro-molds is 215 min (figure 4(c)for a 600 μm-depth) and 189 min (figure 4(d) for a 500 μm-depth).

Based on the model of 3D micro-mold (figure 5), we fabricated the 3D micro-electrode and applied it in micro-EDM. Therefore, the ultimate aim of fabricating the 3D microelectrode is to obtain the 3D micro-mold. In order to investigate the dimensional precision of the 3D micro-mold, we used the laser scanning confocal microscope to measure the main dimensions of the 3D micro-molds. In the process of measurement, the same dimension was measured five times to obtain its mean value. The measurement results and the standard deviations are shown in table 1. The measurement results indicate that the dimensional errors are within 8 μm and this can ensure the geometrical precision of the 3D micro-molds.

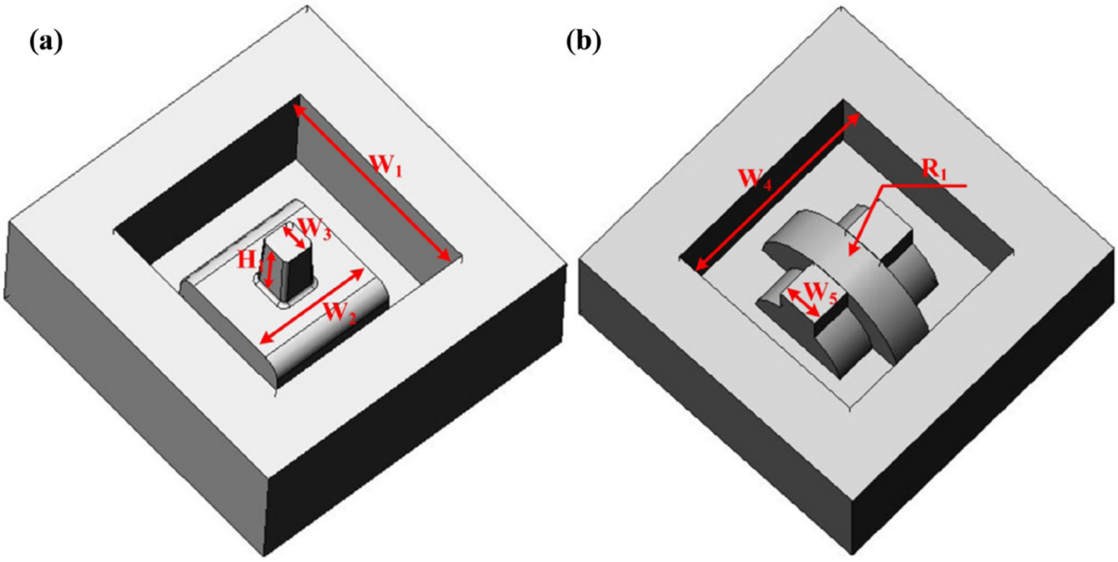

Figure 5. The CAD models of 3D micro-molds: CAD models of 3D micro-molds shown in figure: 4(c); (b) CAD models of 3D micro-molds shown in figure 4(d).

Table 1. Dimensional comparison between machined structures shown in figure 4 and CAD models shown in figure 5.

		Dimensional values (μm)				
Figures	Dimensional symbols	CAD models	Machined structures	Dimensional errors	Standard deviation	Processing time
4(c)	W_1	1000	1004.2	4.2	1.05	215 min
	W_2	600	607.5	7.5	0.22	
	W_3	200	196.2	3.8	0.57	
	H_1	350	346.8	3.2	0.58	
	Depth	600	597.5	2.5	0.42	
4(d)	W_4	1000	1005.3	5.3	0.47	189 min
	W_5	200	198.4	1.6	0.32	
	R_1	400	402.8	2.8	0.31	
	Depth	500	505.3	5.3	0.18	

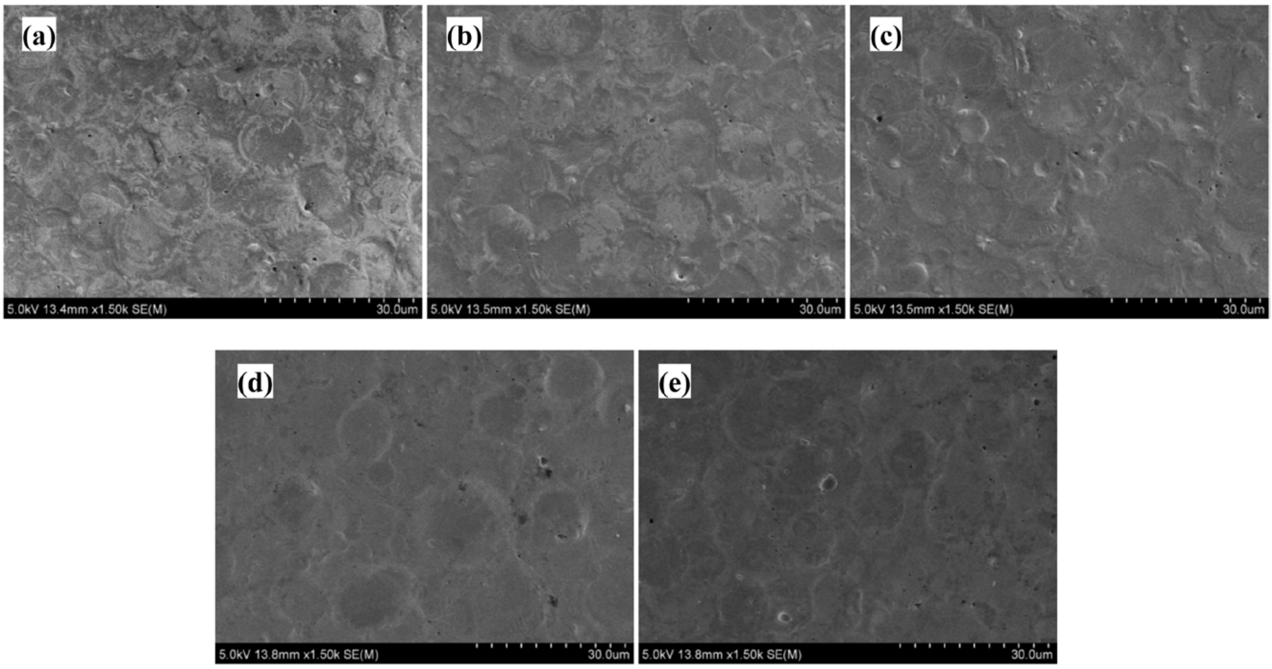

Figure 6. Surface morphology of micro-mold under different processing depths h: (a) $h = 100\ \mu$m; (b) $h = 200\ \mu$m; (c) $h = 300\ \mu$m; (d) $h = 400\ \mu$m; (e) $h = 500\ \mu$m.

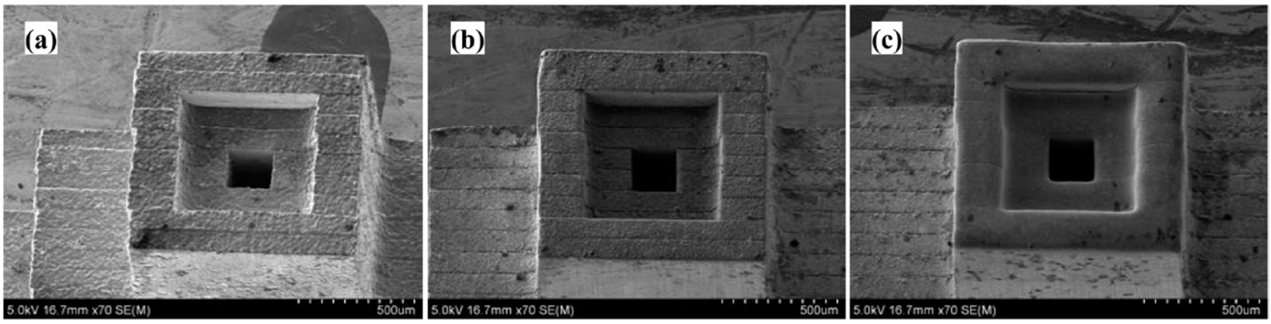

Figure 7. The 3D micro-electrode: (a) 3D micro-electrodes before micro-EDM; (b) 3D micro-electrodes with processing depths of 100 μm; (c) 3D micro-electrodes with processing depths of 500 μm.

4.2. Surface topography of 3D micro-molds

3D micro-molds with different processing depths were observed through SEM and the results are shown in figure 6. The parameters for the micro-EDM are as follows: voltage of 80 V, pulse frequency of 0.2 MHz, pulse width of 800 ns, and pulse interval of 4200 ns. The processing depths of the micro-molds are 100 μm, 200 μm, 300 μm, 400 μm and 500 μm. From the results shown in figure 6, it can be found that discharge craters with a diameter of about 10 μm were produced on the metallic glass surface after micro-EDM. In micro-EDM, gasification was the main style of corrosion removal and gasified erosion resulted in circular discharge craters on the micro-mold surface. With the discharge depth increasing, the craters on the metallic glass surface gradually became shallow, which is an advantage for improving the surface quality of a 3D micro-mold.

Moreover, when the 3D micro-electrode was fabricated, its surface was rough (figure 7(a)). Therefore, in the initial stage of micro-EDM, the micro-mold processed by the 3D micro-electrode has a poor surface quality (figure 6(a)). As shown in table 2, we measured the surface roughness of 3D micro-electrode and 3D micro-mold. From the measurement results, it can be seen that, with processing depth increasing, the surface roughness Ra of the 3D micro-mold was gradually reduced to 0.543 μm from 2.243 μm meanwhile the surface roughness Ra of the 3D micro-electrode was reduced to 0.601 μm from 2.655 μm. After analyzing the aforementioned experimental results, we believe that the surface roughness of 3D micro-electrode can influence the surface roughness of the 3D micro-mold. With the processing depth increasing, the surface of 3D micro-electrode was wearing and became smooth gradually (figures 7(b) and (c)). Consequently, the surface quality of the micro-mold gradually increased.

Table 2. The surface roughness of the micro-mold and micro-electrode under different processing depths.

Depth/μm	100	200	300	400	500
Surface roughness Ra of micro-electrode/μm	2.655	1.908	1.210	1.055	0.601
Surface roughness Ra of micro-mold/μm	2.243	1.823	1.068	0.957	0.543

4.3. EDS analysis on the 3D micro-mold surface

The 3D micro-electrode can be used for 3D micro-EDM with up and down reciprocating machining, which has a high processing efficiency. However, with increased processing depth,chip removal becomes more and more difficult and this could cause carbon deposition in the machining region. Carbon deposition may cause an arc discharge between the electrode and work pieces, resulting in bad surface quality of the micro-mold. As such, this kind of phenomenon should be avoided as far as possible.

To obtain the content of carbon elements, the EDS analysis was carried out on the surface of the micro-molds with different processing depths. The parameters for micro-EDM are as follows: voltage of 80 V, pulse frequency of 0.2 MHz, pulse width of 800 ns and pulse interval of 4200 ns. The processing depths of the micro-molds are 100 μm, 200 μm, 300 μm, 400 μm and 500 μm. The EDS analysis results are shown in figure 8 and table 3.

Based on the experimental results, it can be seen that with the processing depth increasing, the content of carbon elements on the micro-mold surface increased from 0.5% to 5.8%. When the 3D micro-electrode was used for processing metallic glass, the up and down reciprocating machining was carried out in the same position, so as to complete the preparation of the 3D micro-mold. With the increase in the processing depth, the number of electro-discharge machining increased and chip removal became more and more difficult. Under the influence of these factors, the amount of carbon elements in the processing area increased. In this processing condition, carbon elements gradually accumulated on the micro-mold surface, which could result in a high probability of carbon deposition.

4.4. XRD analysis of micro-mold

Metallic glass is isotropic, with no defects such as crystal grains, grain boundaries or dislocation. Moreover, it also has high fracture strength and yield strength. Therefore, it is an ideal kind of plastic material for processing molds. The fracture strength of the $Pd_{40}Cu_{30}P_{20}Ni_{10}$ metallic glass used in this paper is 1326 MPa (sample dimension is 1 mm × 1 mm × 2 mm). In order to study the influence of micro-EDM on metallic glass properties, XRD analysis was

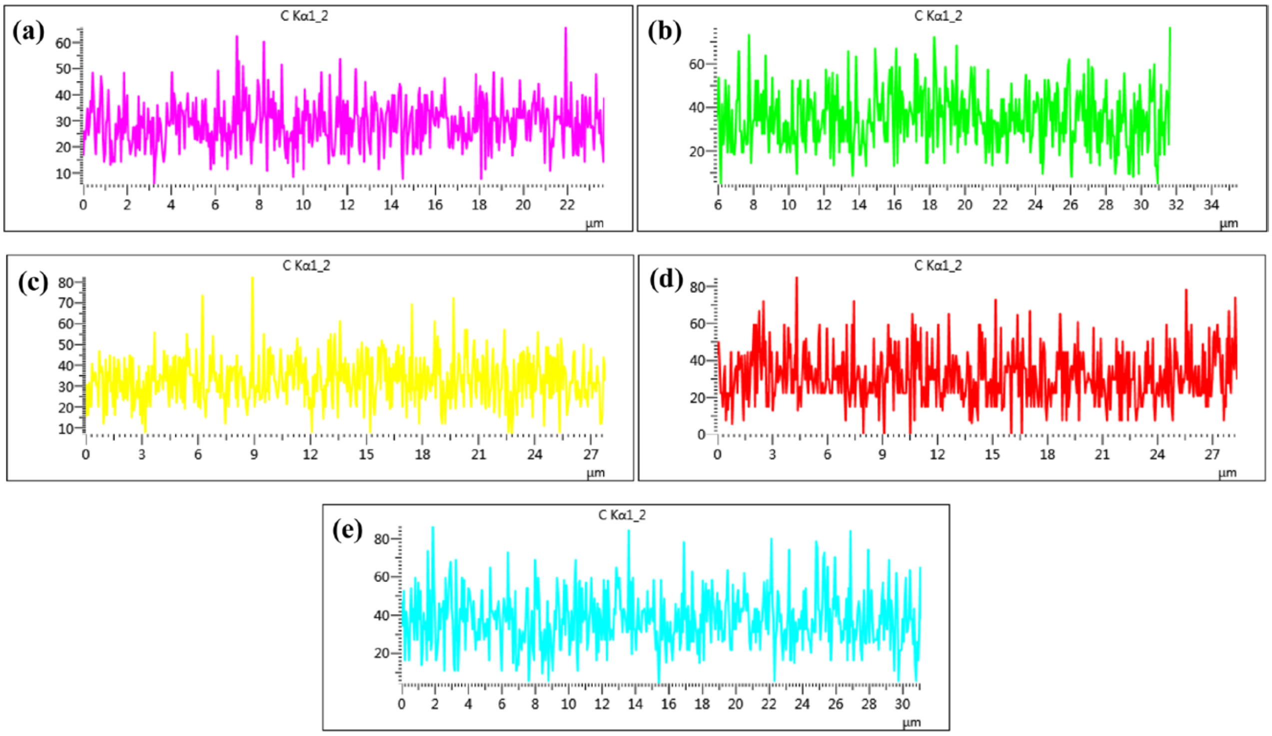

Figure 8. EDS analysis of the micro-mold under different processing depth h: (a) $h = 100$ μm; (b) $h = 200$ μm; (c) $h = 300$ μm; (d) $h = 400$ μm; (e) $h = 500$ μm.

Table 3. The carbon contents of the micro-mold under different processing depths.

Depth/μm	400	500	600	700	800
C/wt%	0.5	1.3	3.5	4.7	5.8

carried out and the results are shown in figure 9. The parameters for micro-EDM are as follows: voltage of 80V, pulse frequency of 0.2 MHz, pulse width of 800 ns, and pulse interval of 4200 ns. The processing depths of the micro-molds are 100 μm, 200 μm, 300 μm, 400 μm and 500 μm.

From the experimental results shown in figure 9, it can be found that the metallic glass material without micro-EDM presents an obviously amorphous diffraction peak (figure 9(a)).With an increased depth of micro-EDM, the Cu_3P phase and $Ni_{12}P_5$ phase were generated in the machining region. This indicates that, under the influence of micro-EDM, the crystallization phenomena occurred in the machining region. During micro-EDM, the discharge channel is formed into an instantaneous temperature field on the surface of the metallic glass. Under the action of the instantaneous temperature field, the metallic glass erodes in the form of gasification and thus results in a new phase on the metallic glass surface.

In order to investigate the influence of micro-EDM on the Cu_3P phase and $Ni_{12}P_5$ phase, we used formula (1) to calculate the relative contents of the Cu_3P phase and $Ni_{12}P_5$ phase in the machining region. As shown in formula (1), I represents the x-ray diffraction intensity of the phase, W represents the relative content of the phase and RIR represents the reference intensity ratio. Through searching PDF cards, it can be obtained that $\mathrm{RIR}_{Cu_3P} = 6.11$ and $\mathrm{RIR}_{Ni_{12}P_5} = 11.83$. The above values were substituted into formula (1) to calculate the relative content of phase and the calculation results are shown in table 4.

$$\begin{cases} K_{Cu_3P}^{Ni_{12}P_5} = \dfrac{\mathrm{RIR}_{Ni_{12}P_5}}{\mathrm{RIR}_{Cu_3P}} \\ W_{Ni_{12}P_5} = \dfrac{I_{Ni_{12}P_5}}{I_{Ni_{12}P_5} + {I_{Cu_3P}}\big/{K_{Cu_3P}^{Ni_{12}P_5}}} \\ W_{Cu_3P} = \dfrac{I_{Cu_3P}}{I_{Cu_3P} + K_{Cu_3P}^{Ni_{12}P_5} \times I_{Ni_{12}P_5}} \end{cases} . \qquad (1)$$

From the calculation results shown in table 4, it can be seen that the relative content of the new phase in the machining region was changed. With an increase in the processing depth, the relative content of $Ni_{12}P_5$ phase gradually decreased from 66.43% to 64.94% and the relative content of Cu_3P phase gradually increased from 33.57% to 35.06%. In micro-EDM, chip removal and heat dissipation becomes more and more difficult when the processing depth increases. This can lead to a temperature rise in the processing area. When the temperature increases to a certain degree, crystallization of the metallic glass can happen. During crystallization of the metallic glass, the $Ni_{12}P_5$ phase is a kind of metastable phase, and its content will gradually decrease. Additionally, the rise of temperature in the processing area accelerates the reaction of copper and phosphorus, forming the Cu_3P phase. Therefore, the relative content of this phase will increase.

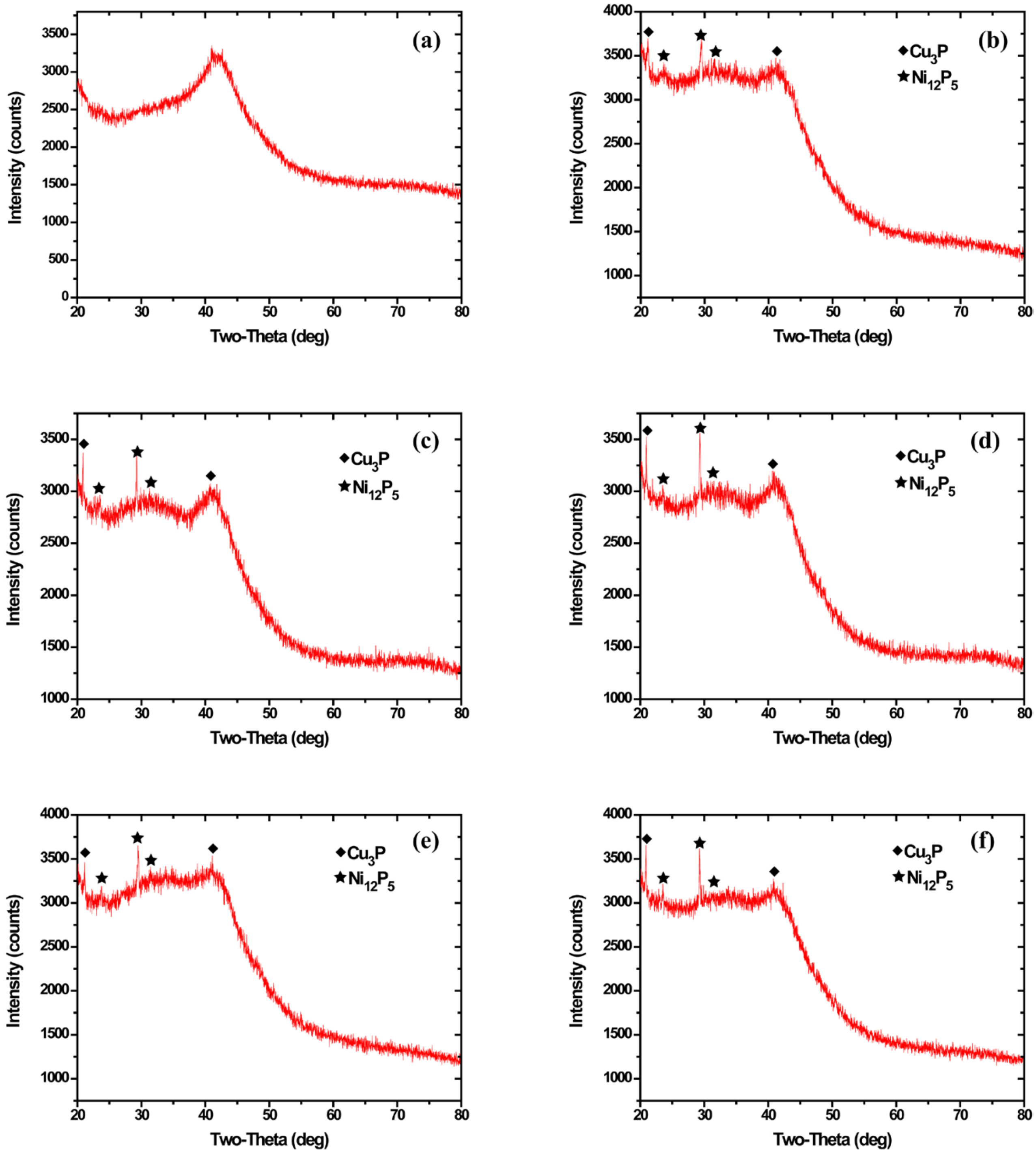

Figure 9. XRD analysis of the micro-mold under different processing depths h: (a) $h = 0\ \mu$m; (b) $h = 100\ \mu$m; (c) $h = 200\ \mu$m; (d) $h = 300\ \mu$m; (e) $h = 400\ \mu$m; (f) $h = 500\ \mu$m.

Table 4. The content of $Ni_{12}P_5$ phase and Cu_3P under different processing depths.

Depth (μm)	Diffraction intensity of $Ni_{12}P_5$ (cd)	Diffraction intensity of Cu_3P (cd)	Relative content of $Ni_{12}P_5$	Relative content of Cu_3P
100	3153	3085	66.43%	33.57%
200	3252	3350	65.27%	34.73%
300	2929	3036	65.13%	34.87%
400	2839	2952	65.06%	34.94%
500	3023	3159	64.94%	35.06%

5. Conclusions

Due to its high fracture strength and yield strength, metallic glass is an ideal material for fabricating 3D micro-molds. For obtaining a 3D micro-mold with better surface quality (slight ridges) and mechanical properties, we fabricated 3D micro-electrodes and applied these to micro-EDM for processing $Pd_{40}Cu_{30}P_{20}Ni_{10}$ metallic glass. Based on the experimental research, our conclusions are as follows:

(1) 3D micro-electrodes were adopted in micro-EDM to obtain 3D micro-molds. Under the voltage of 80 V, pulse frequency of 0.2 MHz, pulse width of 800 ns and pulse interval of 4200 ns, 3D micro-electrodes were used to process $Pd_{40}Cu_{30}P_{20}Ni_{10}$ metallic glass and 3D micro-molds with surface roughness of $Ra = 0.543$ μm were obtained. The 3D micro-mold has a good surface quality and is roughly in line with the design model.
(2) The EDS analysis was carried out on the 3D micro-mold surface and the results show that, with the increase in processing depth, the content of carbon elements on the micro-mold surface increased from 0.5% to 5.8%. Therefore, the probability of carbon deposition in micro-EDM is increased when the processing depth increases.
(3) The XRD analysis was carried out on the 3D micro-mold surface and shows that two kinds of phase (Cu_3P and $Ni_{12}P_5$) appeared in metallic glass after micro-EDM. Furthermore, with the increased depth of micro-EDM, the $Ni_{12}P_5$ phase gradually decreased from 66.43% to 64.94% and the Cu_3P phase gradually increased from 33.57% to 35.06%. The aforementioned experimental results show that, under the influence of micro-EDM, crystallization occurs in the processing area of the metallic glass.

Acknowledgments

This work is supported by the National Natural Science Foundation of China (No. 51405306, No. 51575360, No. 51175348 and No. 51375315), the project is funded by the China Postdoctoral Science Foundation (No. 2014M552233), and the Research and Development Foundation of Science and Technology of Shenzhen (No. JCYJ20140418095735629 and No. JCYJ20150525092941026). The authors are also grateful to colleagues for their essential contribution to the work.

References

[1] Yu Z Y, Masuzawa T and Fujino M 1998 Micro-EDM for three-dimensional cavities-development of uniform wear method *CIRP Ann.-Manuf. Technol.* **47** 169–72
[2] Rajurkar K P and Yu Z Y 2000 3D micro-EDM using CAD/CAM *CIRP Ann.-Manuf. Technol.* **49** 127–30
[3] Tong H, Li Y, Wang Y and Yu D W 2008 Servo scanning 3D micro-EDM based on macro/micro-dual-feed spindle *Int. J. Mach. Tools Manuf.* **48** 858–69
[4] Tong H, Wang Y and Li Y 2008 Vibration-assisted servo scanning 3D micro EDM *J. Micromech. Microeng.* **18** 025011
[5] Peng Z L, Wang Z L, Dong Y H and Chen H 2010 Development of a reversible machining method for fabrication of microstructures by using micro-EDM *J. Mater. Process. Technol.* **210** 129–36
[6] Chi G X, Wang Z L, Xiao K, Cui J Z and Jin B D 2008 The fabrication of a micro-spiral structure using EDM deposition in the air *J. Micromech. Microeng.* **18** 035027
[7] Yu H L, Luan J J, Li J Z, Zhang Y S, Yu Z Y and Guo D M 2010 A new electrode wear compensation method for improving performance in 3D micro EDM milling *J. Micromech. Microeng.* **20** 055011
[8] Nguyen M D, Wong Y S and Rahman M 2013 Profile error compensation in high precision 3D micro-EDM milling *Precis. Eng.* **37** 399–407
[9] Yan M T and Lin S S 2011 Process planning and electrode wear compensation for 3D micro-EDM *Int. J. Adv. Manuf. Technol.* **53** 209–19
[10] Bleys P, Kruth J P and Lauwers B 2004 Sensing and compensation of tool wear in milling EDM *J. Mater. Process. Technol.* **149** 139–46
[11] Li T, Visvanathan K and Gianchandani Y B 2014 A batch-mode micromachining process for spherical structures *J. Micromech. Microeng.* **24** 025002
[12] Chen S T and Chen C H 2015 A novel power source for high-precision, highly efficient micro w-EDM *J. Micromech. Microeng.* **25** 075027
[13] Shibayama T and Kunieda M 2006 Diffusion bonded EDM electrodes with micro holes for jetting dielectric liquid *CIRP Ann.-Manuf. Technol.* **55** 171–4
[14] Xu B, Wu X Y, Lei J G, Cheng R, Ruan S C and Wang Z L 2015 Laminated fabrication of 3D micro-electrode based on WEDM and thermal diffusion welding *J. Mater. Process. Technol.* **221** 56–65
[15] Lei J G, Wu X Y, Xu B, Zhao Z T, Ruan S C and Cheng R 2015 Laminated fitting fabrication of Cu–Sn composite 3D micro electrodes and elimination of ridges on the machined surface of 3D micro-cavities *J. Mater. Process. Technol.* **225** 24–31
[16] Ma J, Zhang X and Wang W H 2012 Metallic glass mold insert for hot embossing of polymers *J. Appl. Phys.* **112** 024506